THE JOURNAL OF PHYSICAL CHEMISTRY B

Article

pubs.acs.org/JPCB

Experimental and Theoretical Observation of Different Intramolecular H-bonds in Lysine Conformations

Bram Boeckx* and Guido Maes

University of Leuven, Celestijnenlaan 200F, 3001 Heverlee, Belgium

Supporting Information

ABSTRACT: Due to the importance of the structure of amino acids for the folding and functionality of proteins, the conformational behavior of lysine has been investigated. Experimental matrix-isolation FT-IR spectra have been recorded. These spectra were interpreted using an extended theoretical DFT and MP2 study. Theoretically, 28 (DFT) and 18 (MP2) conformations were found with $\Delta E < 10$ kJ mol^{-1}. Incorporation of the entropy term changed the relative order of the stability because of the large unfavorable effect of this term for the conformations with one or two intramolecular H-bonds. As a matter of fact, the predicted abundances are strongly temperature dependent. The abundant conformations of lysine at sublimation temperature can be characterized by the type of amino acid backbone and the eventual additional H-bond in four groups. These groups are predicted to be detectable in the matrix, as their abundances are all larger than 5%. The theoretical spectral data of the most abundant conformation of a particular group are used to represent the group. In the matrix-isolation FT-IR spectrum all the important, H-bonded involved modes (ν(OH), ν(NH$_2$), ν(C═O), γ(OH), δ(OH) and γ(NH$_2$)) of the four conformational groups were observed. A linear correlation between the stretching frequency shift ν(XH) and the elongation of the XH distance Δr(XH) in different conformations of lysine and other amino acids has been observed. The experimental frequencies are in good relationship with the theoretically obtained data, which is proven by a mean frequency deviation for the most abundant conformation is 12.6 cm^{-1}.

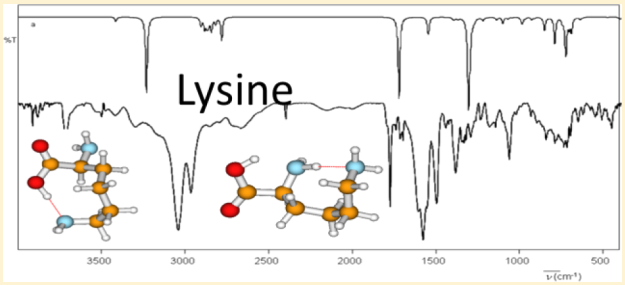

1. INTRODUCTION

The structure of biomolecules determines to a large extend their functionality. For this reason structure determination is of huge importance to understand or predict biological processes.[1] As elementary building blocks of a protein, the conformational behavior and the intrinsic vibrational properties of amino acids have a large influence on the functionality of proteins.[2] It has been demonstrated that the conformation of the side chain of the amino acid residues in a protein generally correspond to the low energy conformations of the amino acid.[3] As a matter of fact, a conformational and vibrational study of amino acids can provide important information for proteins, which are too large for a high-level computational study.

A suitable technique to study conformations and noncovalent bindings is matrix-isolation spectroscopy, supported by theoretical calculations.[4] The obtained vibrational results can also be useful in the search for the origin of life in interstellar space.[5]

The side chain in the amino acid lysine is an aliphatic C4 chain with a basic amino group. Because this NH$_2$ group can be involved in H-bonding,[6] interactions of the amino acid lysine are largely ruled by this.[7−11] This has some importance in biochemical instrumental methods, e.g., the Sänger method for amino acid sequence analysis of polypeptides or ion-exchange chromatography on cation exchange resins, because lysine elutes at large retention times.[12] Lysine is an essential amino acid that must be ingested by food. Lysine sources are protein-rich nutrition such as soy, (red) meat, cheese, cod, sardines, and eggs.[13] Contrary to mammals, plants and bacteria can synthesize lysine starting from aspartic acid.[14] Lysine deficiency causes immunodeficiency as demonstrated with animal tests.[15] From the medical point of view, lysine is used in the treatment of herpes infections.[16]

Due to the basic NH$_2$ group in the side chain, lysine has attracted huge interest. This has resulted in several studies, although very few using moderate to high-level theory combined to experiments. A full structural search of the lysine conformations has been performed by the group of Lin.[17] Compared to earlier studies, this high computational semi-empirical and ab initio study resulted in numerous new lysine structures and a new lowest energy conformation. Not less than 23 conformations of lysine have been found at the DFT-(B3LYP)/6-311++G** level of theory with a relative energy difference smaller than 10 kJ mol^{-1}. The relative MP2/6-311G(2df,p)) energy differences of these conformations appeared all to be smaller than 20 kJ mol^{-1}. Experimentally, several IR studies have been reported on lysine salts[18] and cationized,[19,20] protonated,[21] or adsorbed[22,23] lysine.

Received: July 12, 2012
Revised: September 28, 2012
Published: September 29, 2012

   dx.doi.org/10.1021/jp306916e | J. Phys. Chem. B 2012, 116, 12441−12449

2. METHODOLOGY

2a. Theoretical Methodology. The resulting set of conformations of the study of Leng[17] has been used as starting conformations for optimization calculations. This set was extended with conformations with intermolecular H-bond interactions between the donor and acceptor groups present in lysine. This set has been optimized at the DFT(B3LYP)/6-31++G** and MP2/6-31++G** level of theory.[24−26]

The obtained structures were subjected to a frequency analysis. To correct for the anharmonicity, a zero point energy (ZPE) correction of 0.97 and variable scaling factors were used. These scaling factors depend of the origin of the mode, i.e,. 0.95 for ν(X−H), 0.98 for γ and τ, and 0.975 for all other modes.[27] The PED of each frequency was calculated by a special software package designed by Dr. L. Lapinski (Institute of Physics, Polish Academy of Sciences, Warsaw, Poland).[28] In the theoretical spectra a Lorentzian line shape with a width 2 cm^{-1} was used. The computational calculations were performed using the Gaussian 03 software package[29] available on the high performance computing Linux cluster of the University of Leuven. This computational methodology has been successfully applied previously for the comparison with matrix-isolation FT-IR spectra of similar molecules.[30−36]

2b. Experimental Methodology. The FT-IR spectra of lysine (LYS) in an Ar matrix have been recorded by registration of 128 interferograms with a Bruker IFS66 spectrophotometer at a resolution of 1 cm^{-1}. Lysine was sublimated at 380 K out of a small, homemade furnace and mixed with a large excess of Ar. This gaseous mixture was deposited at a CsI window cooled to 18 K. During this process the pressure in the cryostat was kept at 1.4×10^{-5} mbar.

Using these sublimation parameters, the yield of the amino acid in the matrix was sufficiently to detect the compound and low enough to prevent decomposition of lysine. Lysine (purity >98%) and high purity argon gas (99.99990%) were purchased from Aldrich and Air Liquide, respectively.

3. RESULTS

Lysine has eight degrees of rotational freedom (Figure 1). The backbone of the amino acid gives rise to three internal rotation

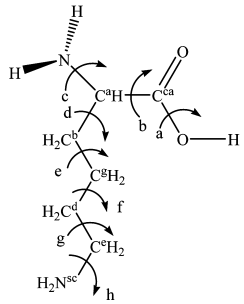

Figure 1. Numbering and possible internal rotational axes (deg) for lysine.

axes, i.e., O=C—OH (a), NC^{α}—C=O (b), and $C^{ca}C^{\alpha}$—NH_2 (c). The side chain gives rise to five additional rotational axes, i.e., NC^{α}—$C^{\beta}C^{\gamma}$ (d), $C^{\alpha}C^{\beta}$—$C^{\gamma}C^{\delta}$ (e), $C^{\beta}C^{\gamma}$—$C^{\delta}C^{\varepsilon}$ (f), $C^{\gamma}C^{\delta}$—$C^{\varepsilon}N^{sc}$ (g), and $C^{\delta}C^{\varepsilon}$—$N^{sc}H$ (h). Full combination of these single-bond rotators results in ($2 \times 6 \times 3 \times 6 \times 3 \times 3 \times 3 \times 3$ =) 17496 theoretical possible structures. This sizable set of structures was optimized by Leng et al.[17] at successive AM1, DFT(B3LYP)/6-31G*, and DFT(BLYP)/6-31++G** levels of theory, and single point MP2 energy calculations were performed at the most stable final geometries. To explore the conformational landscape of lysine, we have started this study from the 23 geometries found by Leng et al. with ΔE_{DFT} < 10 kJ mol^{-1} or ΔE_{MP2} < 20 kJ mol^{-1}. This set was increased with some additional structures with apparently stabilizing H-bond interactions and was then completely optimized at the DFT(B3LYP)/6-31++G** and MP2/6-31++G** levels of theory. Not less than 28 conformations with ΔE_{DFT} < 10 kJ mol^{-1} and 18 with ΔE_{MP2} < 10 kJ mol^{-1} were found. All these conformations were minima, because no imaginary frequencies were observed in the frequency analysis. As previously observed, four different types of amino acid backbone occur. These types are denoted with Roman numerals in Figure 2. All

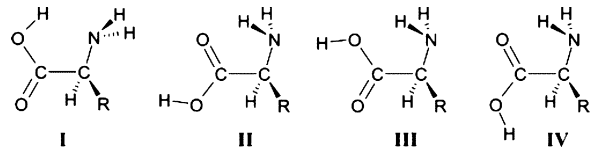

Figure 2. Different types of amino acid backbones.

have a different stabilizing intramolecular H-bond, i.e., OH···N in type I and bifurcated NH_2···O=C, NH_2···O(H), and NH_2···O=C H-bonds in types II, III, and IV, respectively. Furthermore, the COOH group can adopt either an s-cis- (type II and III) or an s-trans- (type I and IV) like conformation.

Compared to the study of Leng,[17] the six most stable MP2 conformations were the same, for the other conformations the order of stability slightly diverse and four additional low-energy conformations were found, i.e., LYS12, LYS16, LYS7, and LYS14. In contrast to the MP2 data the relative energies and the ordering obtained by the DFT method slightly differ compared to Leng. There may be two explanations for this. The conformational freedom of lysine is large and the conformational differences, especially in the position of the CH_2 groups, are small, which results in small energy differences. Furthermore, Leng et al. have obtained the MP2 energies with single point energy calculations in contrast to the optimizations in this study. The optimizations performed in here are also the reason for the relatively smaller energy gap for most of the conformations; e.g., 21 conformations with ΔE_{DFT} < 5 kJ mol^{-1} were found here, whereas Leng et al. have only obtained 8 conformations with ΔE_{DFT} < 5 kJ mol^{-1}.

The NH_2 in the side chain of lysine is a possible H-bond acceptor or, possibly, a very weak H-bond donor, which can give rise to an additional H-bond. The possible additional H-bonds are denoted along with the type of amino acid backbone in Table 1 as OH, NH, C=O, and O(H) for OH···$N^{sc}H_2$, NH_2···N, C=O···H_2N^{sc}, and (H)O···H_2N, respectively.

The optimized MP2 geometries, which are similar to the DFT geometries, of the most stable conformations of lysine are presented in Figure 3. The three most stable conformations have the amino acid backbone type IV, which is characterized by a bifurcated NH_2···O=C intramolecular H-bond and an additional OH···N^{sc} H-bond. Conformations LYS4 to LYS11 have backbone type I, characterized by a OH···N intramolecular H-bond. LYS4 to LYS10 have an additional NH_2···N^{sc} H-bond, whereas LYS11 has an additional C=O···HN^{sc} H-bond. No additional H-bond is found in conformations with backbone type II characterized by a bifurcated NH_2···O=C H-bond and type III stabilized by a NH_2···O(H) H-bond, which explains the

dx.doi.org/10.1021/jp306916e | J. Phys. Chem. B 2012, 116, 12441−12449

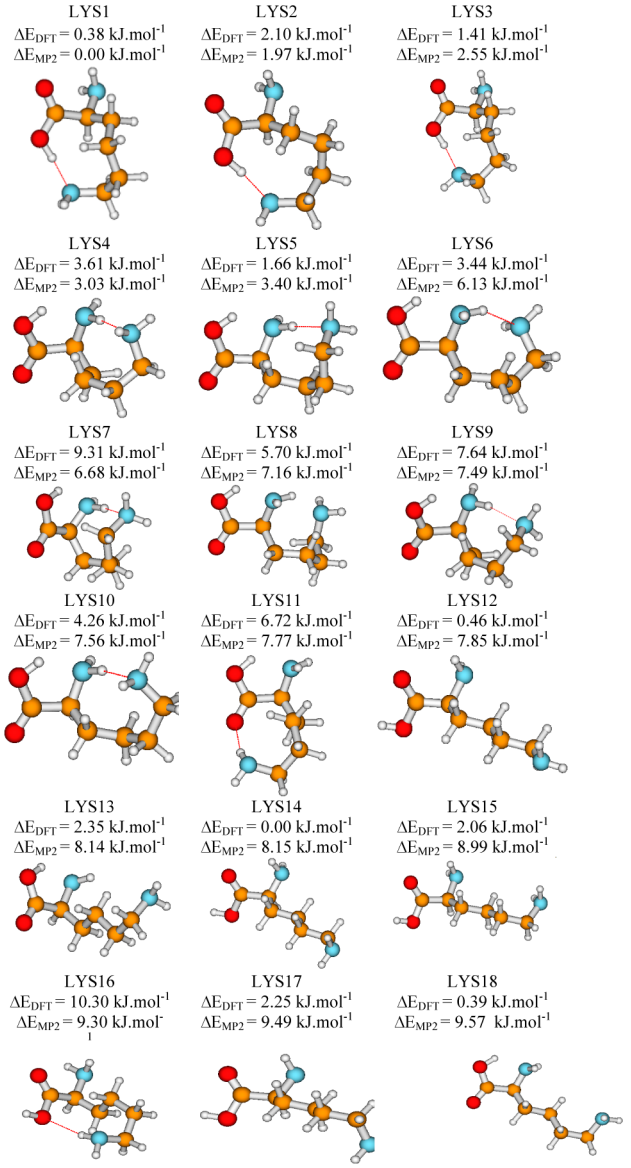

Figure 3. Optimal geometries and relative energies (DFT(B3LYP)/6-31++G** and MP2/6-31++G**) of the most stable conformations of lysine.

large ΔE_{MP2} for LYS12 (ΔE_{MP2} = 7.85 kJ mol^{-1}) and LYS24 (ΔE_{MP2} = 12.32 kJ mol^{-1}), the most stable conformations with amino acid backbone types II and III. The ΔE_{DFT} values for these conformations are considerably smaller, i.e., 0.46 (LYS12) and 1.19 kJ mol^{-1} (LYS26), which can be ascribed to the poor description of the weak interaction by the DFT method.

The thermodynamical MP2 and DFT data for the conformations with ΔE_{MP2} < 10 kJ mol^{-1}, at both room temperature (298.15 K) and the sublimation temperature used (380.00 K), as well as the types of amino acid backbone and the data obtained by Lang et al.[17] are listed in Table 1. A more extended table with the electronic energies, ZPE values, and dipole moments can be found in the Supporting Information. The order of the electronic energies is completely different from the order of the Gibbs free energies. The reason for this is the larger entropy term $T\Delta S°$ for the conformations without an intramolecular H-bond in the side chain. For lysine, the most stable conformations (LYS1 to LYS11) have two intramolecular H-bonds, whereas LYS12−LYS15, LYS17, and LYS18 have only one intramolecular H-bond in the amino acid backbone. The loss of the additional H-bond in the side chain gives rise to a larger, thermodynamically favorable entropy contribution for these conformations. At the sublimation temperature, the entropy contribution $T\Delta S°$ of the conformations without intramolecular H-bond in the side chain becomes larger than the stabilization energy of the H-bond in the lowest-energy conformations. This implies that the lowest energy conformations are not the most abundant at the sublimation temperature. Conformation LYS12 with ΔE_{MP2} = 7.85 kJ mol^{-1} becomes the most abundant ($A^{\%}_{MP2}$ = 17.20%), whereas the lowest MP2 energy conformation (LYS1) has not a considerable abundance ($A^{\%}_{MP2}$ = 3.05%).

The large entropy contribution of some of the conformations has consequences for the equilibrium distributions at different temperatures.[30−36] Because the abundances are clearly affected by the temperature, we have calculated these at various temperatures taking into account an expanded set of 25 conformations, all with ΔE_{MP2} or ΔE_{DFT} < 10 kJ mol^{-1}. The abundance of the most stable conformations (LYS1 to LYS11) decreases rapidly with increasing temperature, whereas the abundance of the conformations without an additional H-bond in the side chain (LYS12−LYS15, LYS17, and LYS18) increases with increasing temperature, as presented in Table 2.

Because the abundances in Table 2 were calculated with a larger set of conformations, these data are more reliable and will therefore be used in the further discussion.

At the sublimation temperature of 380.00 K, six conformations have an MP2 abundance larger than 5%, i.e., LYS4, LYS12−LYS15, and LYS17, which suggests that these conformations are possibly detectable in the matrix IR spectrum. Although all other conformations with an abundance smaller than 5% will not be detectable in the spectrum, these conformations must be taken into account, because the sum of the abundances of all these separate conformations is significant.

The sums of the abundances of the conformations with the same type of backbone and the eventually additional H-bond are presented in Table 3. From this table it appears that, at the sublimation temperature of 380.00 K, the lysine conformations with backbone type II are abundant ($A^{\%}_{MP2}$ = 47.0%), conformations with backbone type I without $A^{\%}_{MP2}$ = 23.9%) and with ($A^{\%}_{MP2}$ = 14.0%) an additional intramolecular NH···N^{sc} H-bond should also be present and conformations of type IV additionally stabilized by an OH···N^{sc} H-bond are possibly detectable ($A^{\%}_{MP2}$ = 6.7%) in the matrix. The abundances of conformations with type III ($A^{\%}_{MP2}$ = 4.0%), type I with an extra C═O···HN^{sc} H-bond ($A^{\%}_{MP2}$ = 1.3%), and type II with an additional (H)O···H$_2$N^{sc} H-bond ($A^{\%}_{MP2}$ = 3.2%) are predicted to be too small to be observable.

As was theoretically demonstrated, six conformations have an abundance larger than 5%. Among these, one (LYS13) has backbone type I, one (LYS4) has type I with an additional NH···N^{sc} H-bond, and four (LYS12, LYS14, LYS15m and LYS17) have backbone type II. These conformations are expected to be present in the low-temperature matrix.

Because the modes of the CH$_2$ groups in the side chain are not suitable to identify different conformations, as previously demonstrated for *N*-acetylalanine,[30] isoleucine,[32] or asparagine,[33] only differences in the amino acid backbone and the eventual additional H-bonds give rise to frequencies differences which can be used to distinguish the different backbone types of lysine. This is clearly demonstrated by Figure 4 which

dx.doi.org/10.1021/jp306916e | J. Phys. Chem. B 2012, 116, 12441−12449

Table 1. DFT(B3LYP)/6-31++G and MP2/6-31++G** Computed Thermodynamical Data for Lysine at 298.15 and 380.00 K: Relative Zero-Point Corrected Energies (ΔE/kJ mol^{-1}), Comparison with Data of Leng et al.,[17] Formation Enthalpies ($\Delta H°$/kJ mol^{-1}), Entropy Contributions ($T\Delta S°$/kJ mol^{-1}), Gibbs Free Energies ($\Delta G°$/kJ mol^{-1}), Rotamerization Constants (K_r), and Abundances (%) of the Conformations with ΔEMP2 < 10 kJ mol^{-1}**

conformation	ΔE^a	ΔE^b	$\Delta H°$	$T\Delta S°$	$\Delta G°$	K_r	%[c]		$\Delta H°$	$T\Delta S°$	$\Delta G°$	K_r	%[c]
					DFT								
					298.15 K[d]						380.00 K[e]		
LYS1	0.00	0.00	0.00	0.00	**0.00**	1.00	0,54	IV OH	0.00	0.00	**0.00**	1.00	0.39
LYS2	1.72	0.96	2.10	1.45	**0.65**	0.77	0.42	IV OH	2.16	1.92	**0.24**	0.93	0.36
LYS3	1.03	1.38	1.37	1.57	**−0.20**	1.08	0.59	IV OH	1.38	2.02	**−0.63**	1.22	0.47
LYS4	3.23	1.51	3.72	4.45	**−0.74**	1.35	0.73	I NH	3.77	5.73	**−1.96**	1.86	0.72
LYS5	1.28	1.30	1.69	3.91	**−2.21**	2.44	1.32	I NH	1.72	5.01	**−3.29**	2.83	1.10
LYS6	3.07		3.50	3.48	**0.03**	0.99	0.54	I NH	3.56	4.49	**−0.93**	1.34	0.52
LYS7	8.93		8.83	1.29	**7.54**	0.05	0.03	I NH	8.84	1.64	**7.19**	0.10	0.04
LYS8	5.32		5.57	2.76	**2.81**	0.32	0.17	I NH	5.61	3.57	**2.05**	0.52	0.20
LYS9	7.26		7.75	3.79	**3.96**	0.20	0.11	I NH	7.77	4.86	**2.91**	0.40	0.15
LYS10	3.88		4.34	3.81	**0.53**	0.81	0.44	I NH	4.36	4.88	**−0.51**	1.18	0.46
LYS11	6.34		7.51	6.17	**1.34**	0.58	0.32	I C═O	7.75	8.14	**−0.38**	1.13	0.44
LYS12	0.08		3.53	13.10	**−9.57**	47.55	25.78	II	4.15	17.41	**−13.25**	66.28	25.71
LYS13	1.97		3.99	9.29	**−5.30**	8.49	4.60	I	4.33	12.22	**−7.90**	12.17	4.72
LYS14	−0.38		3.05	13.09	**−10.04**	57.44	31.14	II	3.71	17.43	**−13.72**	76.88	29.82
LYS15	1.68		4.76	11.88	**−7.11**	17.62	9.56	II	5.40	15.86	**−10.46**	27.37	10.61
LYS16	9.93		12.74	11.89	**0.85**	0.71	0.38	II (O)H	13.34	15.83	**−2.49**	2.20	0.85
LYS17	1.87		5.08	12.56	**−7.48**	20.45	11.09	II	5.74	16.76	**−11.01**	32.64	12.66
LYS18	0.02		2.21	9.94	**−7.73**	22.59	12.25	I	2.56	13.06	**−10.50**	27.77	10.77
					MP2								
					298.15 K[d]						380.00 K[e]		
LYS1	0.00	0.00	0.00	0.00	**0.00**	1.00	6.83	IV OH	0.00	0.00	**0.00**	1.00	3.05
LYS2	1.97	1.72	2.28	1.20	**1.09**	0.64	4.39	IV OH	2.34	1.58	**0.76**	0.79	2.40
LYS3	2.55	3.97	2.84	1.56	**1.28**	0.60	4.07	IV OH	2.83	1.98	**0.85**	0.76	2.33
LYS4	3.03	4.77	3.32	4.36	**-1.05**	1.52	10.41	I NH	3.31	5.55	**-2.24**	2.03	6.20
LYS5	3.40	4.77	3.68	3.68	**0.00**	1.00	6.84	I NH	3.67	4.68	**-1.01**	1.38	4.20
LYS6	6.13	5.19	6.35	2.74	**3.61**	0.23	1.59	I NH	6.37	3.51	**2.85**	0.41	1.24
LYS7	6.68		6.51	0.75	**5.76**	0.10	0.67	I NH	6.53	0.97	**5.55**	0.17	0.53
LYS8	7.16		7.46	3.04	**4.43**	0.17	1.14	I NH	7.52	3.94	**3.58**	0.32	0.98
LYS9	7.49		7.85	3.23	**4.62**	0.15	1.06	I NH	7.85	4.11	**3.74**	0.31	0.94
LYS10	7.56		7.99	3.69	**4.30**	0.18	1.21	I NH	8.01	4.73	**3.28**	0.35	1.08
LYS11	7.77		8.69	5.01	**3.68**	0.23	1.55	I C═O	8.89	6.61	**2.28**	0.49	1.48
LYS12	7.85		11.34	13.12	**−1.78**	2.05	14.01	II	11.96	17.43	**−5.46**	5.64	17.20
LYS13	8.14		10.46	11.66	**−1.20**	1.62	11.08	I	10.80	15.25	**−4.45**	4.09	12.47
LYS14	8.15		11.62	13.01	**−1.38**	1.75	11.93	II	12.28	17.32	**−5.04**	4.93	15.05
LYS15	8.99		12.23	12.75	**−0.52**	1.23	8.43	II	12.86	16.97	**−4.10**	3.67	11.18
LYS16	9.30		11.55	9.48	**2.08**	0.43	2.95	II (O)H	12.06	12.65	**−0.59**	1.21	3.68
LYS17	9.49		12.77	13.09	**−0.32**	1.14	7.76	II	13.42	17.41	**−4.00**	3.54	10.81
LYS18	9.57		11.87	10.60	**1.28**	0.60	4.08	I	12.20	13.88	**−1.68**	1.70	5.19

[a]ZPE corrected energy relative to LYS1: E_{DFT} = −496.875549 au and E_{MP2} = −495.403147 au. [b]Data obtained by Leng et al.[17] [c]Only taking into account the 18 most stable conformations. [d]Relative to LYS1. Absolute values for LYS1: $H°_{DFT}$ = −496.862103 au, $H°_{MP2}$ = −495.390966 au; $TS°_{DFT}$ = 0.048083 au, $TS°_{MP2}$ = 0.047647 au; $G°_{DFT}$ = −496.910187 au, $G°_{MP2}$ = −495.438613 au. [e]Relative to LYS1. Absolute values for LYS1: $H°_{DFT}$ = −496.855809 au, $H°_{MP2}$ = −495.384781 au; $TS°_{DFT}$ = 0.068343 au, $TS°_{MP2}$ = 0.067663 au; $G°_{DFT}$ = −496.924152 au, $G°_{MP2}$ = −495.452444 au.

presents the nearly identical theoretical DFT spectra of LYS12, LYS14, LYS15, and LYS17.

Because the total frequency set for all the 25 conformations in Table 4 would be too large, the most abundant conformation of each type was used to represent the particular group of conformations with the same type of amino acid backbone and eventual additional H-bond, i.e., LYS1 for type IV with an additional OH···N^{sc} H-bond, LYS4 for type I with an additional NH···Nsc H-bond, LYS12 for type II, and LYS13 for type I. The theoretical spectra (Figure 5) exhibit the frequency differences between these conformations. For the ease of spectral discussion we introduce the terms LYStI, LYStII, LYStIVOH, and LYSt1NH, referring to all the conformations with amino acid backbone type I, type II, and type IV with an additional intramolecular OH···N^{sc} H−bond and type I with an additional NH···N^{sc} intramolecular H-bond, respectively.

The overall experimental FT-IR spectrum of lysine in argon is presented in Figure 6. The theoretical spectrum is based on the DFT frequencies of the most stable conformations of each type, taking into account the MP2 abundances at sublimation temperature of all the conformations of that type.

dx.doi.org/10.1021/jp306916e | J. Phys. Chem. B 2012, 116, 12441−12449

Table 2. MP2 Abundances (%) of the 25 Most Stable Lysine Conformations at Different Temperatures

form	type	10 K	100 K	200 K	300 K	380 K	400 K	500 K
LYS1	IV OH	100.0	75.5	23.1	6.1	**2.6**	2.2	1.1
LYS2	IV OH	0.0	8.5	9.5	3.9	**2.1**	1.8	1.0
LYS3	IV OH	0.0	4.8	7.8	3.6	**2.0**	1.8	1.0
LYS4	I NH	0.0	7.2	18.1	9.3	**5.4**	4.8	2.9
LYS5	I NH	0.0	3.6	11.1	6.1	**3.6**	3.2	2.0
LYS6	I NH	0.0	0.1	1.5	1.4	**1.1**	1.0	0.7
LYS7	I NH	0.0	0.0	0.6	0.6	**0.5**	0.4	0.3
LYS8	I NH	0.0	0.0	0.9	1.0	**0.9**	0.8	0.6
LYS9	I NH	0.0	0.0	0.8	1.0	**0.8**	0.8	0.6
LYS10	I NH	0.0	0.0	0.8	1.1	**0.9**	0.9	0.7
LYS11	I CO	0.0	0.0	1.0	1.4	**1.3**	1.2	1.1
LYS12	II	0.0	0.1	5.5	12.8	**14.9**	15.2	15.8
LYS13	I	0.0	0.0	5.0	10.1	**10.8**	10.8	10.4
LYS14	II	0.0	0.0	4.5	10.9	**13.0**	13.3	14.2
LYS15	II	0.0	0.0	2.8	7.7	**9.7**	10.0	11.0
LYS16	IIO(H)	0.0	0.0	1.1	2.7	**3.2**	3.2	3.4
LYS17	II	0.0	0.0	2.3	7.1	**9.4**	9.7	11.1
LYS18	I	0.0	0.0	1.4	3.7	**4.5**	4.6	4.8
LYS19	I	0.0	0.0	0.8	2.5	**3.3**	3.4	3.7
LYS20	I NH	0.0	0.0	0.1	0.2	**0.3**	0.3	0.3
LYS21	I NH	0.0	0.0	0.2	0.4	**0.5**	0.5	0.5
LYS22	I	0.0	0.0	0.3	1.2	**1.6**	1.7	2.0
LYS23	I	0.0	0.0	0.3	1.1	**1.7**	1.8	2.2
LYS24	III	0.0	0.0	0.4	2.4	**4.0**	4.4	5.9
LYS25	I	0.0	0.0	0.3	1.3	**2.0**	2.1	2.7

Table 3. Sum of the Abundances (%) at Sublimation Temperature (380 K), Taking into Account the 25 Most Stable Conformations, of the Conformations with the Same Type of Amino Acid Backbone and an Eventual Additional Intramolecular H-Bond

type[a]	II	I	I NH	IV OH	III	II O(H)	I C=O
$A^{\%}_{MP2}$	47.0	23.9	14.0	6.7	4.0	3.2	1.3

[a]The additional intramolecular H-bonds are denoted as OH, NH, C=O, and O(H) for OH···$N^{sc}H_2$, NH_2···N^{sc}, C=O···HN^{sc}, and (H)O···H_2N^{sc}, respectively.

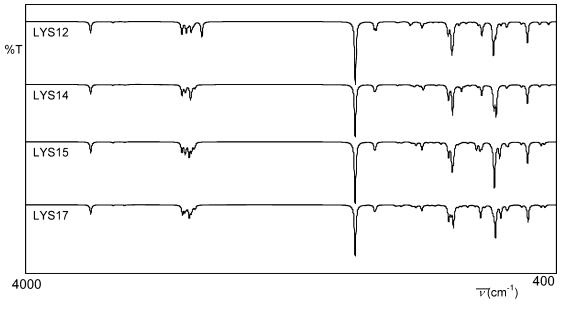

Figure 4. Theoretical (DFT) IR spectra of the most abundant MP2 conformations of lysine with the amino acid backbone type II.

The most elementary observed and the theoretical DFT frequencies, intensities, and PEDs are presented in Table 4. The extended table can be found in the Supporting Information; in that table, all the nonsuitable modes with an intensity smaller than 5 km mol^{-1} are excluded, except for the most abundant conformation LYStII. The spectrum indicates small amounts of water, as can be seen in the absorptions observed in the region 3800−3500 and 1650−1550 cm^{-1}. Because the values of the observed water frequencies are in good agreement with the previously published frequencies for monomeric water in Ar,[37] it may safely be assumed that these impurities have not influenced the vibrational modes of lysine.

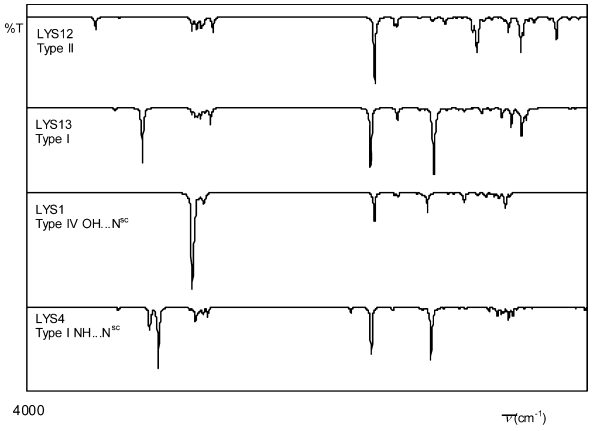

Figure 5. Theoretical (DFT) IR spectra of the most abundant MP2 conformation of each group ($A^{\%}_{MP2}$ > 5%) with the same type of amino acid backbone and eventually an additional H-bond.

The spectrum is discussed for three different spectral regions, i.e., 3600−2350, 2000−1000, and 1000−500 cm^{-1}.

3a. 3600−2350 cm^{-1}. The high frequency region (3600−2350 cm^{-1}) of the FT-IR spectrum of lysine is presented in Figure 7. This region contains the ν(OH) and $\nu(NH_2)$ modes which are important for an experimental discrimination

dx.doi.org/10.1021/jp306916e | J. Phys. Chem. B 2012, 116, 12441−12449

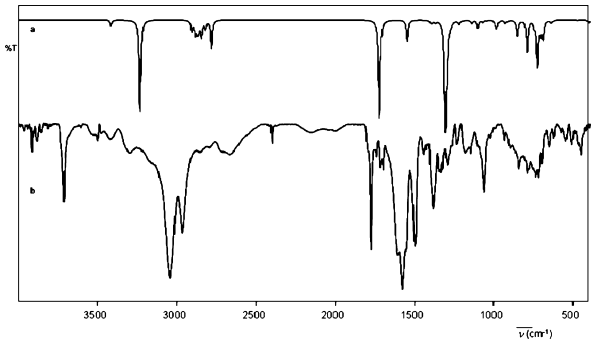

Figure 6. Theoretical DFT (a) and experimental FT-IR (Ar at 18 K) (b) spectrum of lysine.

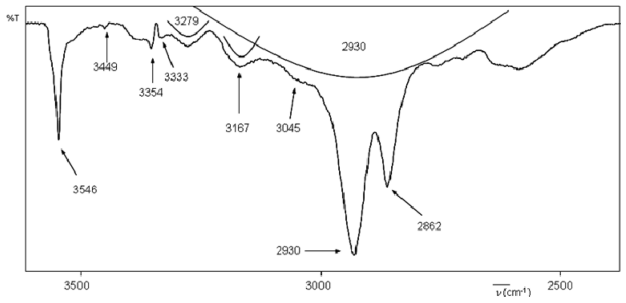

Figure 7. High frequency region (3600−2350 cm^{-1}) of the FT-IR spectrum of lysine in Ar at 18 K.

between conformations of lysine because both the NH_2 and OH groups may be involved in H-bonding.[7]

The ν(OH) mode is the most important vibrational mode as it is involved in an intramolecular H-bond in conformations LYStI (OH···N^{bb}), LYStIVOH (OH···N^{sc}), and LYStINH (OH···N^{bb}), whereas it is not involved in H-bonding in conformation LYStII. These different interactions lead to very different predicted frequencies, i.e., 3559, 3258, 3156, and 2937 cm^{-1} for LYStII, LYStI, LYStINH, and LYStIVOH, respectively. H-bonded modes ν(OH···) are expected to be more intense and broader than free ν(OH) modes. The non H-bonded ν(OH) absorption observed at 3546 cm^{-1} for LYStII is in accordance with the predicted value of 3559 cm^{-1}. The ν(OH···) mode of LYStI is assigned to the broad band at 3279 cm^{-1}, but predicted at 3258 cm^{-1}. The broad band observed at 3167 cm^{-1} can be assigned to the ν(OH···) mode of LYSINH with a theoretical frequency of 3156 cm^{-1}. Finally, the ν(OH···) mode of LYStIVOH is ascribed to the broad band with a maximum at 2930 cm^{-1}. The high predicted intensity (858 $km.mol^{-1}$) of this mode and the intensity contributions of the other ν(OH···) bands and in particular the ν_s and $\nu_{as}(CH_2)$ modes of all the CH_2 groups present explain the large intensity and extent of this band, ranging from ±3400 to ±2300 cm^{-1}.The large contribution to the intensity of this band of the $\nu(CH_2)$ modes is in line with the matrix-isolation FT-IR study of isoleucine.[32]

The observed values for ν(OH) are in line with values of previously studied, similar molecules, as demonstrated in Table 5. Especially the values of nonbonded ν(OH) and the ν(OH···) involved in an OH···N intramolecular H-bond are similar. H-bonds between the OH group and the side chain are stronger bonds, as demonstrated by the larger frequency shift in LYStIVOH and LYStINH. The reason for this is the large flexibility of the side chain in lysine. This allows the more linear geometry in the H-bond. As a matter of fact, the H-bond angle is 173° for both LYStIVOH and LYStINH, which is clearly more linear compared to the values of 127 or 98° for LYStI or isoleucine,[32] respectively. The fact that four different ν(OH) modes are observed implies that conformations of each of the four types are present in the Ar matrix.

Four $\nu(NH_2)$ modes are expected for lysine, i.e., the asymmetric and symmetric stretches for both the backbone

Table 4. Experimentally Observed Frequencies (cm^{-1}), Intensities ($km\ mol^{-1}$), and Theoretical IR Spectral Data (DFT(B3LYP)/6-31++G) for the Most Abundant Conformations of Each Type of Lysine**

		theoretical[a]								
		LYStII		LYStI		LYStINH		LYStIVOH		
experimental		LYS12		LYS13		LYS4		LYS1		
$\bar{\nu}$[b]	I[c]	$\bar{\nu}$	I	$\bar{\nu}$	I	$\bar{\nu}$	I	$\bar{\nu}$	I	PED[d]
3546	s	3559	59							ν(OH) (100)
3279	m			3258	285					ν(OH···) (100)
3167	m					3156	448			ν(OH···) (103)
2930	vs									$\nu^{as}(CH_2)$
								2937	858	ν(OH···) (67)
2862	vs									$\nu^{s}(CH_2)$
1786	sh			1790	307					ν(C═O) (86)
						1786	346			ν(C═O) (85)
1763	vs							1766	326	ν(C═O) (83)
		1763	319							ν(C═O) (87)
1513	s									$\delta(CH_2)$ (100)
1408	w							1425	228	δ(OH···) (72) + $\nu(C^{\alpha}C^{\beta})$ (21)
						1400	390			δ(OH) (67) + ν(C−O) (21)
1114	s	1109	147							δ(OH) (34) + ν(C−O) (20) + $\delta(CH_2)$ (14) + $\delta(N^{sc}H_2)$ (11)
1090		1099	79							δ(OH) (41) + ν(CN) (24) + $\nu(C^{\alpha}H)$ (13)

[a]Variable scaling factors for DFT: 0.95 for (X−H); 0.98 for γ and τ; 0.975 for all other modes. [b]Observed frequency in the matrix-isolation FT-IR spectrum of lysine. [c]Relative experimental intensity denoted as vs (very strong), s (strong), m (medium), w (weak), vw (very weak), and sh (shoulder). [d]Potential energy distribution (%); only contributions >10% are listed.

dx.doi.org/10.1021/jp306916e | J. Phys. Chem. B 2012, 116, 12441−12449

Table 5. Experimental Frequencies of the ν(OH) Mode, $\Delta\nu$(OH) Shift and H-Bond Angle (DFT) in the Lysine Conformations and in the Most Stable H-Bonded and Non H-Bonded Conformations of Other Amino Acids and *N*-Acetylated Amino Acids

	experimental[a]			
	$\nu(OH)^{free}$ (cm^{-1})	$\nu(OH)^{bonded}$ (cm^{-1})	$\Delta\nu$ (cm^{-1})	H-bond angle (deg_
LYStII	3559			
LYStI		3279	−280	127
LYStIVOH		3167	−392	173
LYStINH		2937	−622	173
proline[38]	3559	3025	−534	
cysteine[39]	3570−3540	3330−3270	±265	
glycine[40,41]	3560	3200	−360	
isoleucine[32]	3565	3251	−314	98
alanine[42]	3560	3193	−367	
N-acetylproline[35]	3561	2950	−611	
N-acetylcysteine[36]	3561	3120	−441	
N-acetylglycine[31]	3546	3005	−541	
N-acetylalanine[30]	3544	3085	−459	

[a]Observed in an Ar matrix.

(bb) NH_2 and the side chain (sc) NH_2 group. The NH_2 group of the amino acid backbone is involved in a weak $NH_2\cdots O{=}C$ H-bond in conformations with backbone types II and IV. This is clearly reflected by the theoretical frequency values. The $\nu_{as}(NH_2)$ and $\nu_s(NH_2)$ of LYStI are predicted at 3436 and 3349 cm^{-1}, respectively. The first one is observed at 3449 cm^{-1}. The $\nu(N^{bb}H_2)$ modes of the other conformations are slightly red-shifted due to the weak $NH_2\cdots O{=}C$ interaction to 3415−3392 cm^{-1} and to 3328 and 3316 cm^{-1} for the asymmetric and symmetric modes, respectively. The ν(NH···) mode of LYStINH involved in an $N^{bb}H\cdots N^{sc}$ intramolecular H-bond causes a much stronger red shift to 3211 cm^{-1}. The broad shoulder at 3045 cm^{-1} might be assigned to this mode. Because the intensities of most of the ν(NH) modes are rather small except for LYStINH, the assignments in Table 5 are somewhat tentative.

Because the symmetric as well as the asymmetric CH_2 stretching vibrations of $C^{\beta}H_2$, $C^{\gamma}H_2$, $C^{\delta}H_2$, and $C^{\varepsilon}H_2$ are strongly coupled, we cannot distinguish between these modes. The PEDs mentioned in Table 5 are the sum of the contributions of all the CH_2 groups. Two intense bands at 2931 and 2862 cm^{-1}, superimposed on the broad ν(OH···) band, can be assigned to $\nu^{as}(CH_2)$ and $\nu^{s}(CH_2)$, respectively.

The shifted frequencies due to H-bonding used above as tools for the identification of the different conformations are further analyzed. Not only are the frequencies shifted, but also the distance r(HX) increases by H-bond formation. This parameter can be quantified by the distance increase, which is the difference between the bond length in conformation with and without a H-bond. The correlation between this distance increase and the $\Delta\nu$(XH) frequency shift in 27 conformations of isoleucine,[32] phenylalanine, or lysine is presented in Figure 8. A linear relation is observed for the different types of H-bond donors (NH and OH). This relation is independent of the nature of the H-bond and can be expressed by

$$\Delta\nu(\mathrm{XH})\ (\mathrm{cm}^{-1}) = -20123\Delta r(\mathrm{XH})\ (\text{Å}) - 27$$

The R^2 value of this equation is 0.924.

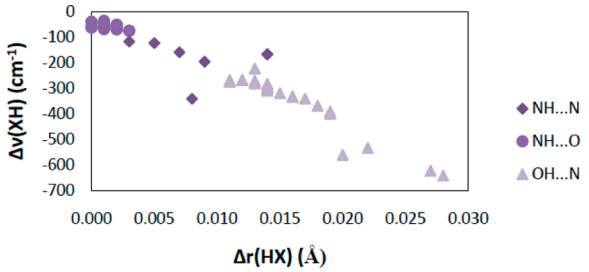

Figure 8. Correlation between the stretching frequency shift ν(XH) and the elongation of the XH distance Δr(XH) in different conformations of isoleucine, phenylalanine, and lysine.

3b. 2000−1000 cm^{-1}. The spectral region 2000−1000 cm^{-1} is shown in Figure 9. The important ν(C═O) modes are

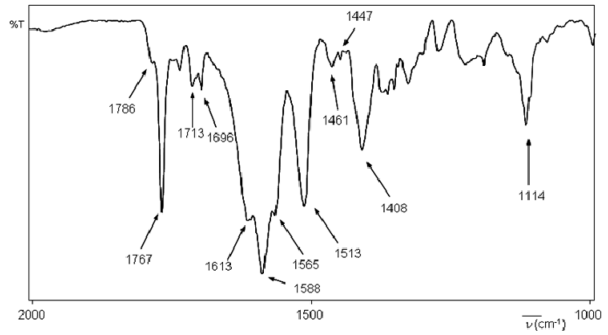

Figure 9. Frequency region 2000−1000 cm^{-1} of the FT-IR spectrum of lysine in Ar at 18 K.

predicted at 1790 and 1786 cm^{-1} for LYStI and LYStINH, whereas the frequencies are slightly red-shifted to 1763 and 1766 cm^{-1} for LYStII and LYStIVOH, respectively. The reason for this shift is obviously the weak H-bond interaction $NH_2\cdots O{=}C$ in the latter forms. In the experimental spectrum a strong band is observed at 1763 cm^{-1} with a high frequency shoulder at 1786 cm^{-1}. According to the predicted values, the first band can be assigned to ν(C═O) of LYStII and LYStIVOH and the second to ν(C═O) of LYStI and LYStINH. A doublet band is observed at 1713 and 1696 cm^{-1}, but no bands are predicted here. This doublet band is most probably an overtone of the broad band experimentally observed at 855 cm^{-1}.

The frequencies of the $\delta(NH_2)$ modes are predicted between 1649 and 1615 cm^{-1}. The absorption due to the bending $\nu 2$ mode of the water impurities does not allow us to correctly analyze this spectral region. Therefore, the assignment of these modes to the triplet band observed at 1614, 1588, and 1565 cm^{-1} is rather tentative.

The bands observed at 1513, 1461, and 1447 cm^{-1} can be assigned to the $\delta(CH_2)$ modes predicted in this region for all the conformations present. Due to the strong coupling of these modes we cannot distinguish between the scissor and the rocking modes of CH_2 and just refer to both these modes as $\delta(CH_2)$. Furthermore, due to the weak intensities and frequency differences between the different conformations, the assignments of these $\delta(CH_2)$ modes in Table 5 are tentative.

The δ(OH) mode is important for detection of conformations with H-bonding of the OH group. This mode is predicted to be blue-shifted due to intramolecular H-bonding toward the

dx.doi.org/10.1021/jp306916e | J. Phys. Chem. B 2012, 116, 12441−12449

higher wavenumbers 1386, 1400, and 1425 cm^{-1} for conformations LYStI, LYStINH, and LYStIVOH, respectively. In the spectrum, this δ(OH) mode can be observed at 1373 cm^{-1} for the first and at 1408 cm^{-1} for the latter two conformations. The δ(OH) mode of LYStII, which is not involved in any H-bond, has significant potential energy contribution to the predicted modes at 1109 and 1099 cm^{-1} and is experimentally observed at 1114 cm^{-1}.

3c. 1000−500 cm^{-1}. The low frequency region (1000−500 cm^{-1}) of the matrix FT-IR spectrum of lysine is presented in Figure 10. The important γ(OH) mode is situated in this region. The predicted frequencies of this mode are clearly affected by intramolecular H-bonding. The γ(OH) not involved in any H-bond for LYStII is predicted at 596 cm^{-1}, whereas the theoretical values of the H-bond involved γ(OH···) modes are 884 cm^{-1} for LYStI, 903−934−946 cm^{-1} for (different PED contributions of γ(OH···) for these moedes) LYStINH, and the extremely high value of 1047 cm^{-1} for LYStIV.

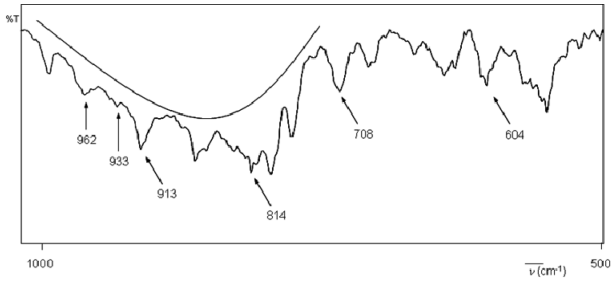

Figure 10. Low frequency region (1000−500 cm^{-1}) of the FT-IR spectrum of lysine in Ar at 18 K.

A very broad band is observed between ±1000 to ±700 cm^{-1}. This band clearly originates from the H-bonded γ(OH···) modes, whereas the band at 604 cm^{-1} can be assigned to γ(OH) of LYStII.

The $\gamma(NH_2)$ mode is also situated in this region. In LYStINH, the NH_2 group of the backbone is H-bonded to the N atom of the side chain in an intramolecular NH···N^{sc} H-bond, whereas the NH_2 group in LYStIVOH and LYStII is involved in a weak intramolecular NH_2···O═C interaction. These interactions are reflected by the predicted frequencies, i.e., 974, 923, and 905 cm^{-1} for LYStINH, LYStIVOH, and LYStII and 820 cm^{-1} for LYStI. According to these values, the observed bands at 962, 933, 913, and 814 cm^{-1} can be assigned to the respective $\gamma(NH_2)$ modes. The first three bands are broad, and the last is a narrow band observed as a superposition on the broad γ(OH···) band.

The mean frequency deviation between the predicted DFT frequencies and the experimentally observed frequencies of LYStII is 12.6 cm^{-1}, based on the 42 assigned vibrational modes. This value is comparable to similar molecules studied with this technique, i.e., asparagine[33] (7.6 cm^{-1}), isoleucine[32] (4.7 cm^{-1}), *N*-acetylproline[35] (12.8 cm^{-1}), *N*-acetylglycine[31] (10.2 cm^{-1}), *N*-acetylalanine[30] (9.5 cm^{-1}), or *N*-actelylcysteine[36] (5.5 cm^{-1}). This demonstrates that the combined matrix-isolation FT-IR DFT methodology is suitable to study complex intramolecular H-bond containing conformations.

4. CONCLUSIONS

The theoretical exploration of the conformational landscape of lysine resulted in 28 conformations with ΔE_{DFT} < 10 kJ mol^{-1} and 18 conformations with ΔE_{MP} < 10 kJ mol^{-1}. This large amount of low energy conformations can be explained by the small energy differences due to the small conformational differences in the aliphatic side chain. The observed energy differences between the different conformations are largely due to the additional intramolecular H-bond caused by the NH_2 group in the side chain.

The ordering of the Gibbs free energies is not in line with that of the electronic energies. The reason for this is the unfavorable entropy contribution of the conformations with an intramolecular H-bond. This is especially important for lysine because, due to the side chain, some of the conformations have two intramolecular H-bonds. As a consequence, the predicted abundances are strongly dependent on the temperature.

The abundant conformations of lysine can be characterized by the type of amino acid backbone and the eventual additional H-bond in four types, i.e., type II, type I, type I with an additional NH···N^{sc} H-bond, and type IV with an additional OH···N^{sc} H-bond. These groups are predicted to be detectable in the matrix, as their abundances are all larger than 5% at the sublimation temperature of 380 K. The theoretical spectral data of the most abundant conformation of a particular type are used to represent the group.

In the matrix-isolation FT-IR spectrum all the important, H-bonded involved modes (ν(OH), $\nu(NH_2)$, ν(C═O), γ(OH), δ(OH), and $\gamma(NH_2)$) of the four conformational types were observed. We were not able to perform an experimental estimation of the rotamerization constant for lysine because the H-bond involved modes gave rise to broadening in the regions where possible useful, separated bands belonging to a particular group are located.

A linear correlation between the stretching frequency shift, $\Delta\nu$(XH), and the elongation of the XH distance, Δr(XH), in different conformations of lysine and other amino acids has been observed.

The obtained mean frequency deviation between predicted and observed frequencies for the most abundant conformation is 12.6 cm^{-1}.

■ ASSOCIATED CONTENT

Ⓢ Supporting Information

Tables of energies, dipole moments, frequencies, intensities, and IR data. This material is available free of charge via the Internet at http://pubs.acs.org.

■ AUTHOR INFORMATION

Corresponding Author

*E-mail: boeckx@hotmail.com.

Notes

The authors declare no competing financial interest.

■ ACKNOWLEDGMENTS

B.B. thanks the Department of Chemistry of the University of Leuven for financial support. The calculations were conducted utilizing the high performances computational resources provided by the University of Leuven, http://ludit.kuleuven.be/hpc.

■ REFERENCES

(1) Dokholyan, N. V.; Borreguero, J. M.; Buldyrev, S. V.; Ding, F.; Stanley, H. E.; Shakhnovich, E. I. Identifying Importance of Amino Acids for Protein Folding from Crystal Structures. In *Methods in Enzymology, Macromolecular Crystallography, Part D*; Charles, W. C., Ed.; Academic Press: New York, 2003; Vol. 374, pp 616−638.

(2) Luscombe, N. M.; Laskowski, R. A.; Thornton, J. M. *Nucleic Acids Res.* **2001**, *29*, 2860−2874.
(3) Petrella, R. J.; Karplus, M. *Proteins: Struct. Funct., Bioinf.* **2004**, *54*, 716−724.
(4) Garand, E.; Kamrath, M. Z.; Jordan, P. A.; Wolk, A. B.; Leavitt, C. M.; Mccoy, A. B.; Miller, S. J.; Johnson, M. A. *Science* **2012**, *335*, 694−698.
(5) Snyder, L. E.; Hollis, J. M.; Suenram, R. D.; Lovas, F. J.; Brown, L. W.; Buhl, D. *Astrophys. J.* **1983**, *268*, 123−128.
(6) Berg, J. M.; Tymoczko, J. L.; Struyver, L. *Biochemistry*; Freeman: New York, 2002.
(7) Stearns, J. A.; Seaiby, C.; Boyarkin, O. V.; Rizzo, T. R. *Phys. Chem. Chem. Phys.* **2009**, *11*, 125−132.
(8) Dos, A.; Schimming, V.; Huot, M. C.; Limbach, H. H. *J. Am. Chem. Soc.* **2009**, *131*, 7641−7653.
(9) Dos, A.; Schimming, V.; Tosoni, S.; Limbach, H. H. *J. Phys. Chem. B* **2008**, *112*, 15604−15615.
(10) Copley, R. R.; Barton, G. J. *J. Mol. Biol.* **1994**, *242*, 321−329.
(11) Ahn, J. H.; Lee, H. J.; Lee, E. K.; Yu, H. K.; Lee, T. H.; Yoon, Y.; Kim, S. J.; Kim, J. S. *Biol. Chem.* **2011**, *392*, 347−356.
(12) Moore, S.; Spackman, D. H.; Stein, W. H. *Anal. Chem.* **1958**, *30*, 1185−1190.
(13) University of Maryland Medical Center Lysine. http://www.umm.edu/altmed/articles/lysine-000312.htm, accessed 2012.
(14) Purdue University Lysine biosynthesis and catabolism. http://www.hort.purdue.edu/rhodcv/hort640c/branch/br00007.htm, accessed 2012.
(15) Chen, C.; Sander, J. E.; Dale, N. M. *Avian Diseases* **2003**, *47*, 1346−1351.
(16) Griffith, R. S.; Norins, A. L.; Kagan, C. *Dermatologica* **1978**, *156*, 257−267.
(17) Leng, Y.; Zhang, M.; Song, C.; Chen, M.; Lin, Z. *J. Mol. Struct. (THEOCHEM)* **2008**, *858*, 52−65.
(18) Petrosyan, A. M.; Ghazaryan, V. V. *J. Mol. Struct.* **2009**, *917*, 56−62.
(19) Bush, M. F.; Oomens, J.; Williams, E. R. *J. Phys. Chem. A* **2009**, *113*, 431−438.
(20) Bush, M. F.; Forbes, M. W.; Jockusch, R. A.; Oomens, J.; Polfer, N. C.; Saykally, R. J.; Williams, E. R. *J. Phys. Chem. A* **2007**, *111*, 7753−7760.
(21) Vaden, T. D.; De Boer, T. S. J. A.; MacLeod, N. A.; Marzluff, E. M.; Simons, J. P.; Snoek, L. C. *Phys. Chem. Chem. Phys.* **2007**, *9*, 2549−2555.
(22) Kitadai, N.; Yokoyama, T.; Nakashima, S. *J. Colloid Interface Sci.* **2009**, *329*, 31−37.
(23) Kitadai, N.; Yokoyama, T.; Nakashima, S. *J. Colloid Interface Sci.* **2009**, *338*, 395−401.
(24) Becke, A. D. *Phys. Rev. A* **1988**, *38*, 3098−3100.
(25) Lee, C. T.; Yang, W. T.; Parr, R. G. *Phys. Rev. B.* **1988**, *37*, 785−789.
(26) Moller, C.; Plesset, M. S. *Phys. Rev.* **1934**, *46*, 618−622.
(27) Van Bael, M. K.; Smets, J.; Schoone, K.; Houben, L.; McCarthy, W.; Adamowicz, L.; Nowak, M. J.; Maes, G. *J. Phys. Chem. A* **1997**, *101*, 2397−2413.
(28) Rostkowska, H.; Lapinski, L.; Nowak, M. J. *Vibr. Spectrosc.* **2009**, *49*, 43−51.
(29) Frisch, M. J.; Trucks, G. W.; Schlegel, H. B.; Scuseria, G. E.; Robb, M. A.; Cheeseman, J. R.; Montgomery, J. A.; Vreven, T.; Kudin, K. N.; Burant, J. C.; Millam, J. M.; et al. *Gaussian 03*, Revision B.05; Gausian, Inc.: Wallingford, CT, 2003.
(30) Boeckx, B.; Maes, G. *Spectrochim. Acta Part A* **2012**, *86*, 366−374.
(31) Boeckx, B.; Maes, G. *J. Phys. Chem. A* **2012**, *116*, 1956−1965.
(32) Boeckx, B.; Nelissen, W.; Maes, G. *J. Phys. Chem. A* **2012**, *116*, 3247−3258.
(33) Boeckx, B.; Maes, G. *J. Biophys. Chem.* **2012**, *165*−*166*, 62−73.
(34) Muzomwe, M.; Boeckx, B.; Maes, G.; Kasende, O. E. *S. Afr. J. Chem.* **2011**, *64*, 23−33.
(35) Boeckx, B.; Ramaekers, R.; Maes, G. *J. Biophys. Chem.* **2011**, *159*, 247−256.
(36) Boeckx, B.; Ramaekers, R.; Maes, G. *J. Mol. Spectrosc.* **2010**, *261*, 73−81.
(37) Bentwood, R. M.; Barnes, A. J.; Orville-Thomas, W. J. *J. Mol. Spectrosc.* **1980**, *84*, 391−404.
(38) Stepanian, S. G.; Reva, I. D.; Radchenko, E. D.; Adamowicz, L. *J. Phys. Chem. A* **2001**, *105*, 10664−10672.
(39) Dobrowolski, J. C.; Jamroz, M. H.; Kolos, R.; Rode, J. E.; Sadlej, J. *ChemPhysChem* **2007**, *8*, 1085−1094.
(40) Stepanian, S. G.; Reva, I. D.; Radchenko, E. D.; Rosado, M. T. S.; Duarte, M. L. T. S.; Fausto, R.; Adamowicz, L. *J. Phys. Chem. A* **1998**, *102*, 1041−1054.
(41) Boeckx, B.; Maes, G. *J. Phys. Chem. B* **2012**, *116*, 11890−11898.
(42) Stepanian, S. G.; Reva, I. D.; Radchenko, E. D.; Adamowicz, L. *J. Phys. Chem. A* **1998**, *102*, 4623.